--Supplementary Information--

Copper sensing function of *Drosophila* metal-responsive transcription factor-1 is mediated by a tetranuclear Cu(I) cluster

Xiaohua Chen[1,5], Haiqing Hua[2,5], Kuppusamy Balamurugan[2,5], Xiangming Kong[1], Limei Zhang[3], Graham N. George[3], Oleg Georgiev[2], Walter Schaffner[2], and David P. Giedroc[1,4]

[1] Department of Biochemistry and Biophysics, Texas A&M University, College Station, TX 77843-2128 USA

[2] Institute of Molecular Biology, University of Zurich, Winterhurerstrasse 190, 8057 Zurich, Switzerland

[3] Department of Geological Sciences, University of Saskatchewan, Saskatoon, S7N 5E2, Canada

[4] Department of Chemistry, Indiana University, Bloomington, IN 47405-7102 USA

[5] These authors contributed equally to this work.

Supplementary Methods

Supplementary Table SI
EXAFS curve-fitting results

Supplementary Table SII
$^{1}H_{N}$, ^{15}N, $^{13}C\alpha$ and $^{13}C\beta$ resonance assignments for Cu_4 C-dMTF_81 (pH 6.2, 25 ºC)

Supplementary Figure S1
C-dMTF_81 binds Zn(II), Cd(II) and Co(II) to form 1:1 protein-metal complexes

Supplementary Figure S2
Cu(I) binding by C-dMTF_81

Supplementary Figure S3

MALDI-TOF mass spectra obtained upon mixing one mol•equiv of Cu(I) to C-dMTF_81 (**A**) or two mol•equiv of Cu(I) to C-dMTF_131 (**B**)

Supplementary Figure S4
^{1}H-^{15}N NMR spectroscopy of C-dMTF_81 in the presence and absence of 4.0 mol•equiv of Cu(I)

Supplementary Figure S5
NMR analysis of Cu_4 C-dMTF_81

Supplementary Figure S6
Quantitation of select ^{1}H-^{15}N HSQC crosspeak intensities as a function of Cu(I):C-dMTF_81 molar ratio

Supplementary Methods

Copper sensitivity assays in S. cerevisiae

These experiments were carried out essentially as previously described (1) with a wild-type strain, DTY7, the *ace1*Δ strain, DTY59, and the plasmids p426*GPD* and p426*GPD-pccs+IV* were kindly provided by Dr. Simon Labbé, Université de Sherbrooke. Briefly, PCR products obtained from amplification of specific regions of the *dMTF-1* gene were cloned between the *Spe*I and *Sma*I sites of p426*GPD*. DTY59 strain was transformed with empty vector p426*GPD* (negative control), p426*GPD-pccs+IV* (positive control) or p426*GPD* containing the indicated dMTF domain: p426*GPD–dMTF*, p426*GPD –dMTF-*Δ*(C+MT)*, p426*GPD–dMTF-*Δ*MT*, p426*GPD–(C+MT)*, p426*GPD–dMTF-C* and p426*GPD–dMTF-MT* and spotted onto a complete synthetic medium containing the indicated CuSO4 concentration (from 0-500 μM). The wild-type strain DTY7 was transformed with p426*GPD* alone as a second positive control. The cells were allowed to grow for 7 days at ambient temperature.

Plasmids, protein expression and purification

A bacterial expression plasmid, pETC-dMTF_81, was constructed to express residues 499-579 of *Drosophila* MTF-1, denoted C-dMTF_81, by amplifying a DNA fragment via the polymerase chain reaction using the cDNA plasmid pChdMTF-1 as the template. The PCR primers incorporated *Nco*I and *Bgl*II restriction endonuclease sites, to permit subcloning of the PCR product directly into *Nco*I/*Bam*HI-restricted pET-3d. Recombinant C-dMTF–81 was inducibly expressed in *E. coli* BL21(DE3) transformed with pETC-dMTF_81 to ampicillin resistance on Luria broth containing 100 μg/mL ampicillin at 37ºC to an OD_{600} = 0.6, and the cells were harvested. Frozen cells from 9 L of growth media were resuspended in lysis buffer (50 mM MES, pH 6.3, 100 mM NaCl, 2 mM DTT) and lysed by sonification. Polymin P [10% (w/v), pH

7.9] was added to the low-speed cellular supernatant to a final concentration of 0.4% to precipitate the nucleic acids. The solution was centrifuged, and solid ammonium sulfate was added to the supernatant to a saturation of 65% on ice to precipitate C-dMTF and remove the PEI. The ammonium sulfate pellet was resuspended in same MES buffer and dialyzed exhaustively against the buffer to remove ammonium sulfate. The dialyzed fraction was applied to an AKTA purifier fitted with anion exchange column equilibrated with the same MES buffer at 5.0 mL/min, and the columns were washed with 6 column volumes of the same buffer. C-dMTF, an acidic protein binds to the Q column, and is eluted by applying a linear gradient of MES buffer to 1.0 M NaCl. The proteins are 95% homogenous after this step and were confirmed by N-terminal sequencing and MALDI-TOF mass spectroscopy. 131-residue (residues 499-629) and 51-residue (residues 529-569) dMTF fragments were subcloned and purified in an analogous way. The isolated proteins were subject to exhaustive dialysis against MES buffer (10 mM MES pH 6.3; 0.1M NaCl) in an anaerobic glovebox (Vacuum-Atmospheres, Inc.). The free thiols content for each protein was determined by DTNB reaction as described (2) with all proteins containing greater than 95% reduced cysteines. The protein concentration was determined by absorbance at 280 nm with $\varepsilon_{280} = 5600\ M^{-1}\ cm^{-1}$.

MALDI-TOF mass spectrometry

MALDI-TOF mass spectra were recorded on Applied Biosystems Voyager-DE STR mass spectrometer. The Cu-C-dMTF_81 sample was prepared 1:1 ratio with sinapic acid and spotted on a stainless steel plate (1 μL spot) and allowed to dry, then placed into the MALDI instrument. This sample was run under the following conditions: 25,000 Volts of accelerating voltage; 90% Grid; 400 ns delay time; accumulated 100 laser shots for each spectrum. The 2:1 Cu-C-dMTF_131 sample was run by the Mass Spectrometry Laboratory at Indiana University under

similar conditions.

Circular dichroism spectroscopy

Far-UV CD spectra were collected on an AVIV 62DS spectropolarimeter operating at 25.0 ± 0.1 ºC in a 1 mm rectangular cell with apo-dMTF_131, Cu_4-dMTF_131, and Zn-dMTF_131 concentration of 10 μM in 6 mM sodium phosphate, pH 7.0, 0.20 M NaF (3). Typical acquisition parameters were 2 s time constant, 1 nm bandwidth, 10 replicates. All spectra were base-line-corrected by subtraction of an averaged scan derived from buffer, and are presented in units of mean residue ellipticity, $[\Theta]_{MRE}$ (deg cm^2 $dmol^{-1}$).

X-ray absorption spectroscopy (XAS) data collection and analysis

XAS measurements were conducted at the Stanford Synchrotron Radiation Laboratory (SSRL) with the SPEAR 3 storage ring containing between 80-100 mA at 3.0 GeV essentially as previously described (4). Cu K-edge data were collected on the beamline 9-3 operating with a wiggler field of 2 T and employing a Si(220) double-crystal monochromator. Beamline 9-3 is equipped with a rhodium-coated vertical collimating mirror upstream of the monochromator and a bent-cylindrical focusing mirror (also rhodium-coated) downstream of the monochromator. Harmonic rejection was accomplished by setting the energy cutoff angle of the mirrors to 12 keV. The incident and transmitted X-ray intensities were monitored using Nitrogen-filled ionization chambers, and X-ray absorption was measured as the Cu Kα fluorescence excitation spectrum using an array of 30 germanium detectors. During data collection, samples were maintained at a temperature of approximately 10 K using an Oxford instruments liquid helium flow cryostat. For each sample, 3 to 4 35-min scans were accumulated, and the energy was calibrated by reference to the absorption of a standard copper metal foil measured

simultaneously with each scan, assuming a lowest energy inflection point of the copper foil to be 8980.3 eV. The energy threshold of the extended X-ray absorption fine structure (EXAFS) oscillations was assumed to be 8995.3 eV. The extended x-ray absorption fine structure (EXAFS) oscillations $\chi(k)$ were quantitatively analyzed by curve-fitting using the EXAFSPAK suite of computer programs with *ab initio* theoretical phase and amplitude functions calculated using the program FEFF version 8.2 (5). No smoothing, filtering, or related operations were performed on the data.

NMR spectroscopy

NMR spectra were acquired at 25ºC on a Varian INOVA 600 spectrometer equipped with a triple resonance probe and X,Y,Z gradient unit. The NMR sample was made in 10 mM MES (pH 6.3) and 0.1 M NaCl and contained 200 μM for ^{1}H-^{15}N HSQC and 700 μM for ^{1}H-{^{15}N} ssNOE experiments. Pulsed-field gradients were incorporated into these experiments for coherence selection and suppression of the solvent water signal. ^{1}H-{^{15}N} steady-state NOE (ssNOE) spectra were obtained by recording spectra with and without the use of ^{1}H saturation for 5 s before the start of experiment and measuring the relative peak intensities. All data were processed and analyzed using NMRPipe and NMRDraw (6).

Supplementary Table SI EXAFS curve-fitting parameters

Cu-S			Cu-N/O			Cu···Cu			
N	*R (Å)*	σ^2*(Å^2)*	*N*	*R(Å)*	σ^2*(Å^2)*	*N*	*R(Å)*	σ^2*(Å^2)*	*F*
C-dMTF_81 with 1 mol equiv Cu(I)									
3	**2.259(2)**	**0.0035(1)**				**2**	**2.698(3)**	**0.0051(2)**	**0.214**
						1	**2.822(7)**	**0.0055(2)**	
2	2.264(2)	0.0010(1)	1	2.029(9)	0.0020(8)	3	2.721(1)	0.0093(2)	0.218
3	2.248(2)	0.0036 (2)				1	2.707(2)	0.0028(2)	0.251
C-dMTF_81 with 3.5 mol equiv Cu(I)									
3	**2.260(1)**	**0.0036(1)**				**2**	**2.709(2)**	**0.0043(1)**	**0.133**
						1	**2.840(4)**	**0.0047(1)**	
2	2.264(1)	0.0009(1)	1	2.019(6)	0.0025(5)	1	2.730(2)	0.0087(1)	0.144
3	2.247(2)	0.0035(1)				1	2.714(2)	0.0023(1)	0.187

Note: *N*, coordination number; *R*, interatomic distance; σ^2, the Debye-Waller factor (the mean square deviation in interatomic distance); the fit-error function, *F*, is defined as $[\Sigma(\chi_{expt}-\chi_{calc})^2k^6/\Sigma(\chi_{expt})^2k^6]^{½}$, where the summations are over all data points included in the refinement; and the values in parentheses are the estimated standard deviations (precision) obtained from the diagonal elements of the covariance matrix. The parameters highlighted in **bold** represent the best fits to each data set (see text for discussion).

Supplementary Table SII $^{1}H_N$, ^{15}N, $^{13}C\alpha$ and $^{13}C\beta$ resonance assignments for Cu_4 C-dMTF_81 (pH 6.2, 25ºC)

Residue #	$^{13}C\alpha$	$^{13}C\beta$	^{15}N	$^{1}H_N$
Ala542	52.94	19.11		
Asp543	56.07	29.48	118.5	8.158
Ala544	52.86	19.54	125.3	8.395
Gly545	45.59	-	107.7	8.467
Ile546	59.97	40.86	117.1	7.799
Cys547	**60.85**	**33.54**	**b**	**b**
Asn548	52.32	38.95	130.4	8.697
Cys549	**60.99**	**35.55**	**122.1**	**8.440**
Thr550	64.02	68.57	120.2	8.651
Asn551	53.10	37.99	122.5	8.404
Cys552	**63.99**	**34.54**	**121.8**	**8.520**
Lys553	54.71	32.54	132.1	8.869
Cys554	**62.71**	**36.27**	**123.8**	**8.529**
Asp555	53.30	41.16	121.9	8.684
Gln556	58.25	28.56	b	b
Thr557	63.37	69.79	113.3	8.615
Lys558				
Ser559				
Cys560	**58.64**	**36.76**	**b**	**b**
His561	57.00	26.43	115.0	8.734
Gly562	45.27	-	111.0	8.851
Gly563			c	c
Asp564	52.70	39.76	117.3	8.392
Cys565	**61.99**	**35.40**	**121.7**	**7.273**
Gly566	46.59	-	c	c
Ala567	53.32	19.43	123.5	7.950
Ala568				

[a] virtually identical resonance assignments are observed for GB1-T2Q_aa27 residues 543-567 under the same solution conditions. [b] chemical exchanged broadened under these conditions. [c] corresponds to one of the two remaining unassigned Gly spin systems observed in GB1-T2Q_aa27. No entry, unassigned.

Supplementary Figure S1 C-dMTF_131 binds Zn(II), Cd(II) and Co(II) to form 1:1 protein-metal complexes. (**A**) An anaerobic titration of Zn(II) into a mixture of mag-fura-2 (16.3 μM) and apo-C-dMTF_131 (15.8 μM). The solid lines through the data represent the results of a simultaneous nonlinear least squares fit of both data sets to a 1:1 binding model with K_{Zn} optimized to 2.1 (±1.3) x 10^{10} M^{-1} and K_{Zn} for mag-fura-2 fixed at 5.0 x 10^{7} M^{-1}. This value represents a lower limit for K_{Zn} since Zn(II) binds stoichiometrically ($\geq 10^{10}$ M^{-1}) (7). Conditions: 20 mM MES, pH 6.3, 0.1 M NaCl, 22 ºC. (**B**) An anaerobic titration of 0.5 mM Cd(II) into 24 μM apo-C-dMTF_131 monitored at 240 nm (*inset*) with the full saturated spectrum shown in the main body of the figure. A fit to a 1:1 binding model is shown (*solid line*): n=0.81, K_{Cd}=2.6 x 10^{6} M^{-1}. Conditions: 20 mM HEPES buffer, pH 7.4, 0.1 M NaCl, 22 ºC. (**C**) An anaerobic titration of 1.5 mM Co(II) into 240 μM apo-C-MTF_131 monitored at 680 nm (*inset*), with the saturated molar absorptivity spectrum shown in the main body of the figure. A fit to a 1:1 binding model is shown (*solid line*): n=0.87, K_{Co}=1.3 x 10^{6} M^{-1}, also a lower limit for K_{Co} since Co(II) binds stoichiometrically under these conditions. Conditions: 20 mM HEPES, pH 7.4, 0.1 M NaCl, 22 ºC. These data taken collectively suggest that Zn(II) and Co(II) form a saturating 1:1 complexed with C-dMTF_131 while adopting an average S_3(N/O) coordination geometry, as revealed by the intensity and wavelength maximum of the Co(II) electronic absorption spectrum in the visible and near ultraviolet regions (8,9). In contrast, Cd(II) forms appears to form a 1:1 complex with an average S_4 coordination geometry, based on the intensity of the ε_{240} nm transition (7).

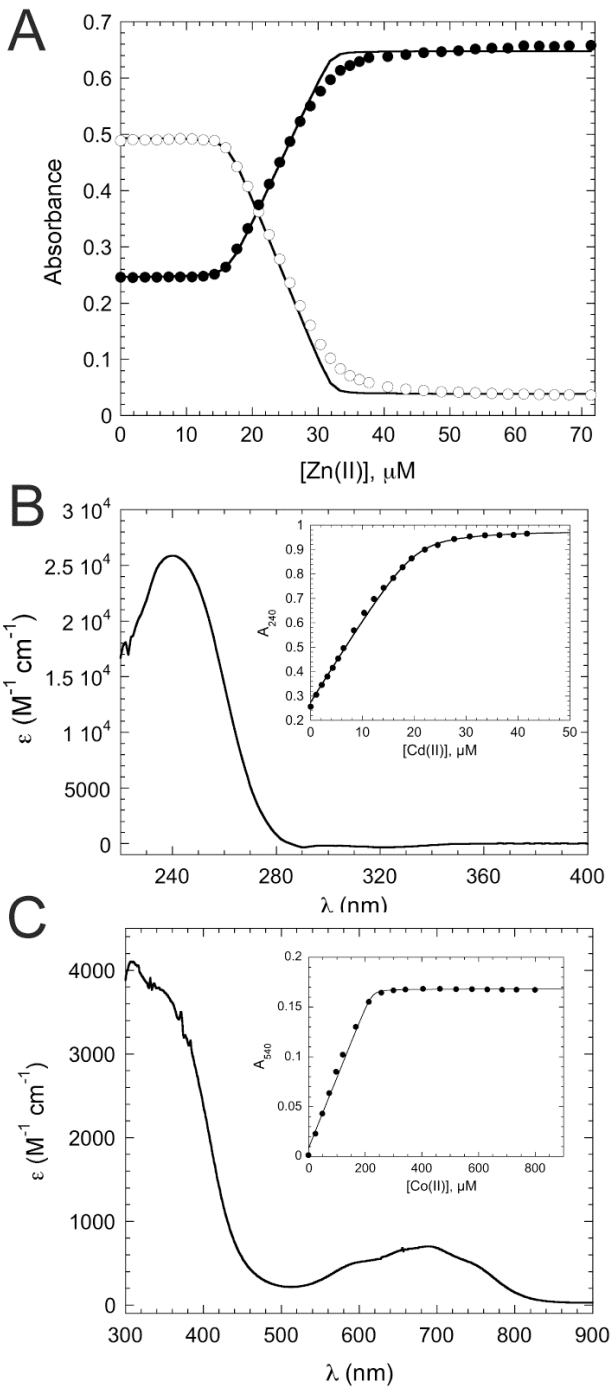
A
Absorbance
[Zn(II)], μM
B
ε (M-1 cm-1)
λ (nm)
A240
[Cd(II)], μM
C
ε (M-1 cm-1)
λ (nm)
A540
[Co(II)], μM

Supplementary Figure S2 Cu(I) binding by C-dMTF_81 is unaffected by preincubation with 4.0 mol•equiv of Zn(II) (**A**) and readily competes with the high affinity Cu(I) chelator BCS for Cu(I) (**B**). (**A**) Absorbance at 265 nm plotted as a function of Cu(I):C-dMTF_81 ratio in the absence (*black filled circles*; data taken from Fig. 4A) and presence of 4.0 mol•equiv of Zn(II). (**B**) Titration of a mixture of 100 µM BCS and 30 µM Cu(I) with the indicated concentration of C-dMTF_81 (from 5-50 µM). Conditions: pH 6.0, 22 ºC.

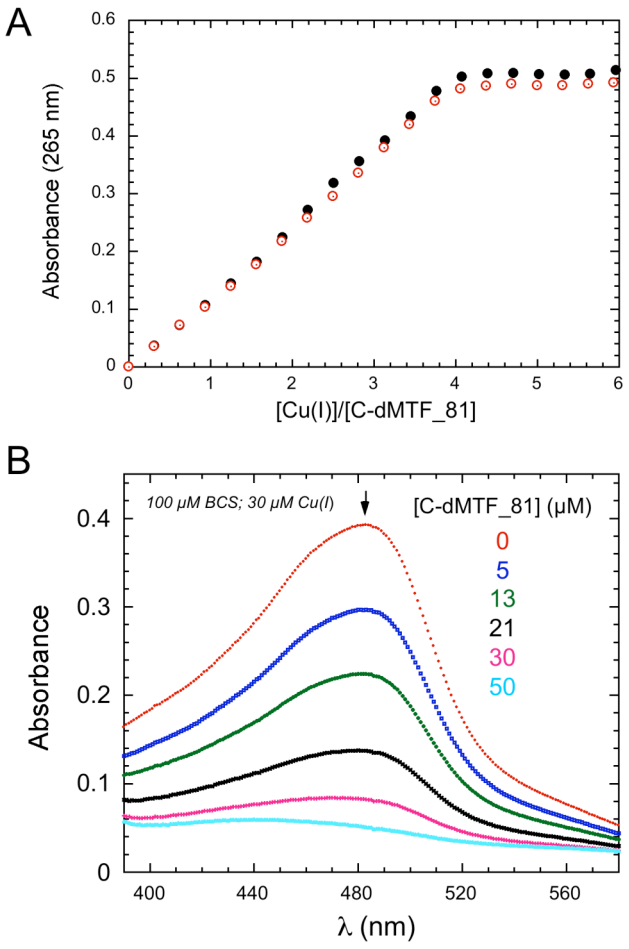

Supplementary Figure S3 MALDI-TOF mass spectra obtained upon mixing one mol•equiv of Cu(I) to C-dMTF_81 (**A**) or two mol•equiv of Cu(I) to C-dMTF_131 (**B**). (**A**) The major peak represents apo-C-dMTF_81 (expected, 8543.3 D) while the minor peak at larger mass represents Cu_4-C-dMTF_81 (expected mass, 8797.4 D) or a Δ=254.1 D (Δ_{obs}=251.1 D). Cooperative assembly of a Cu_4 complex is expected to yield a 3:1 peak area ratio similar to what is observed. (**B**) A comparison of the apo C-dMTF_131 mass spectrum (*blue*) with the spectrum obtained on mixing 2 mol•equiv Cu(I) (*red*) reveals a mass shift of 257.5 D (Δ=254.1 D expected). Cooperative assembly would yield a 1:1 peak area ratio similar to that observed.

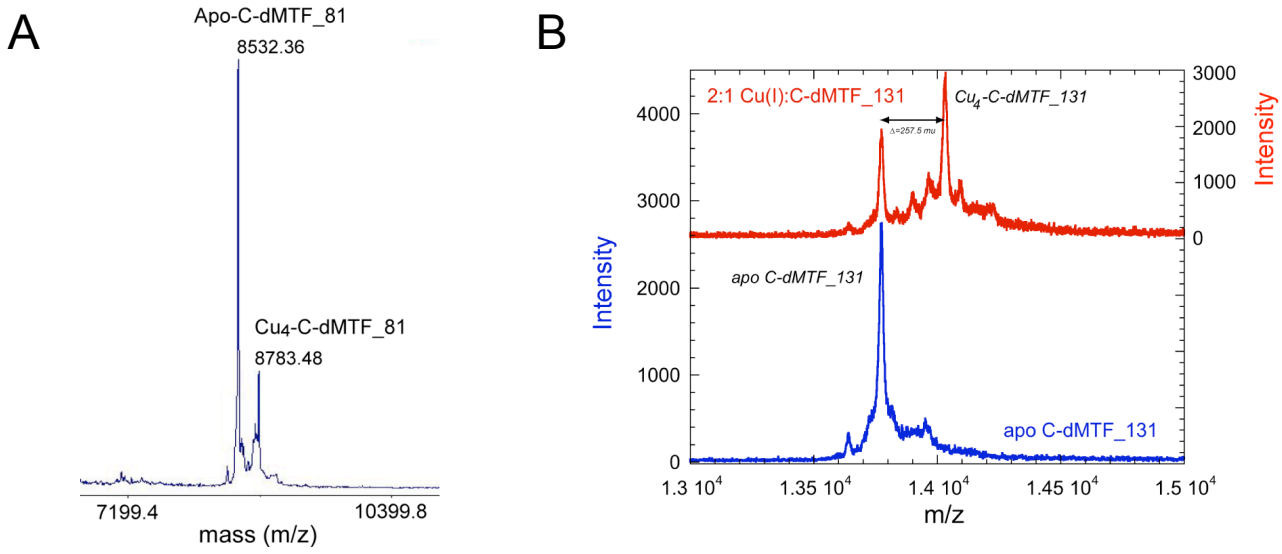

Supplementary Figure S4 ^{1}H-^{15}N NMR spectroscopy of C-dMTF_81 in the presence and absence of 4.0 mol•equiv of Cu(I). *Top*, amino acid sequence of the Cys-rich region in dMTF-1 is shown, with Cys residues (*bold*) and selected residues for which assignments have been made (*red*) are highlighted. (**A**) Full ^{1}H-^{15}N HSQC spectra of apo (*blue contours*) and Cu_4 (*red contours*). (**B**) ^{1}H-{^{15}N}-heteronuclear NOE spectra acquired with a 5 s presaturation. Those crosspeaks with negative intensities are shaded *red*, while those with positive intensities are shaded *blue*. Note that those resonances that shift on Cu-binding (panel *A*) also have positive ^{1}H-{^{15}N}-heteronuclear NOEs, indicated of a folded structure. The boxed region is expanded in Fig. 7 in the main text. Conditions: pH 6.2, 25ºC, 600 MHz.

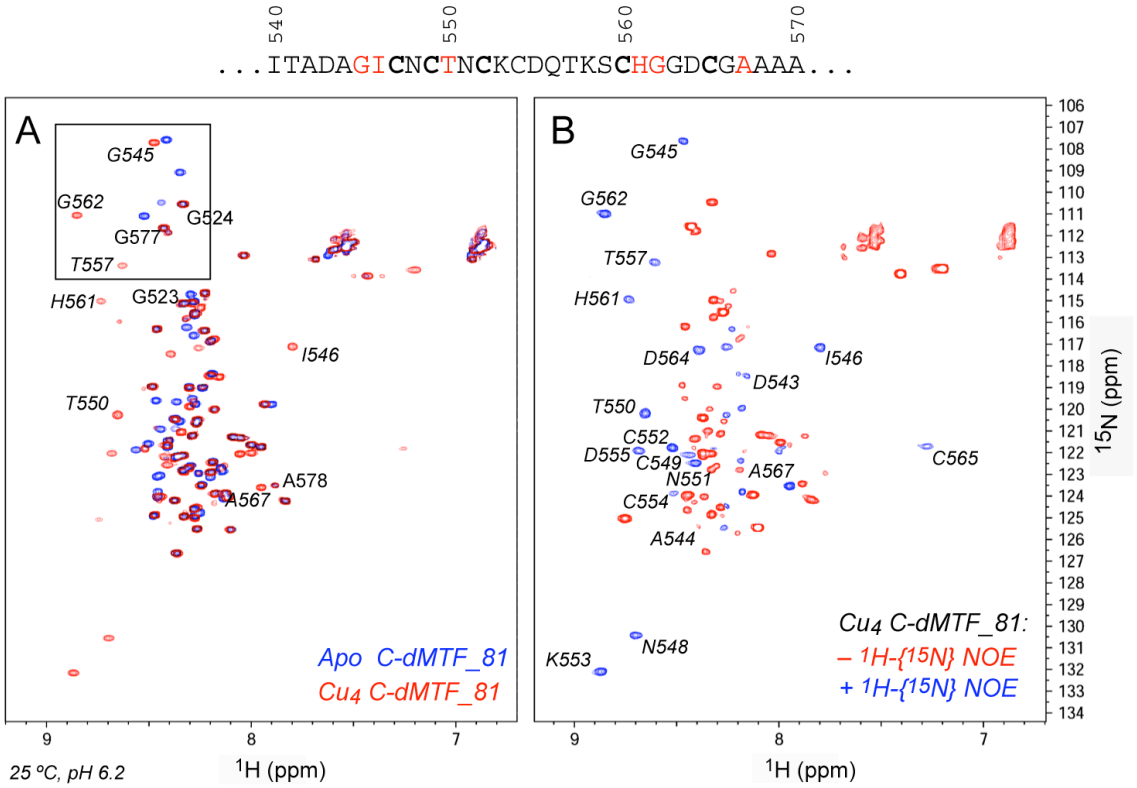

Supplementary Figure S5. *Top panel*, the presence of an observable or assignable amide proton is indicated by a *filled* circle. *Bottom panel*, ssNOE values for individual amide resonances of C-dMTF_81 are shown with the range, where indicated, derived from the analysis of C-dMTF_81 and C-dMTF_131 spectra (see Materials and Methods). The assigned amide resonances from Ile546-Ala567 are characterized by an average ssNOE value of ≈0.87 consistent with a folded structure around the Cu(I) ions, with immediately adjacent N-terminal residues exhibiting lower ssNOE values, indicative of considerable flexibility at the N-terminus of the folded domain.

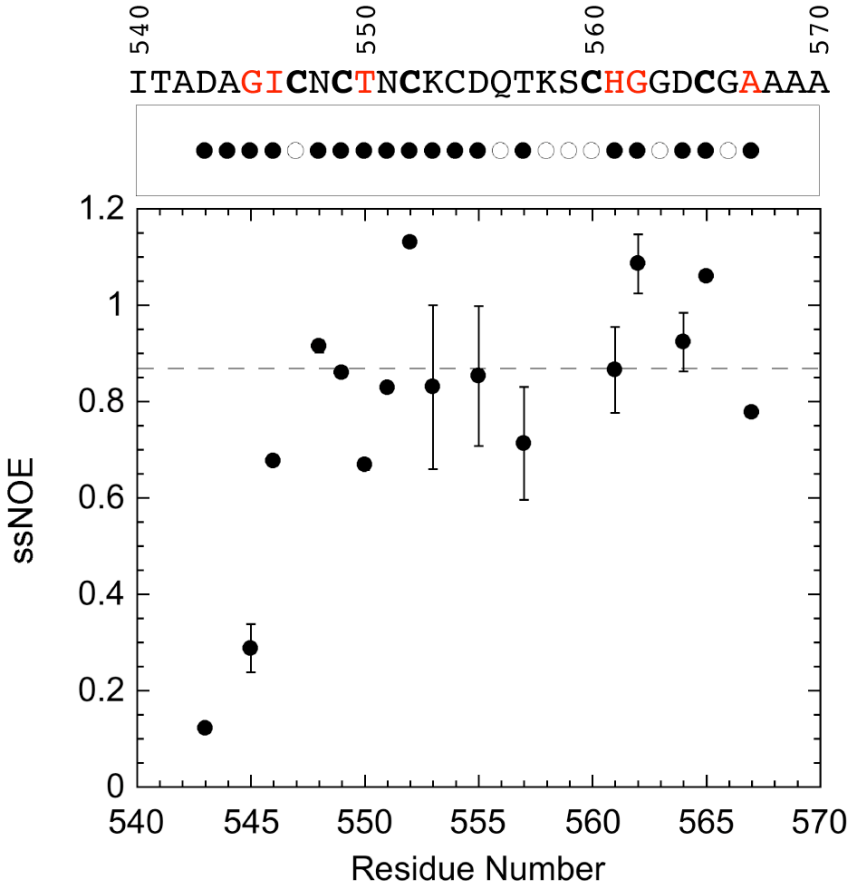

Supplementary Figure S6 Quantitation of select ^{1}H-^{15}N HSQC crosspeak intensities as a function of Cu(I):C-dMTF_81 molar ratio (see Fig. 7 for actual spectra).

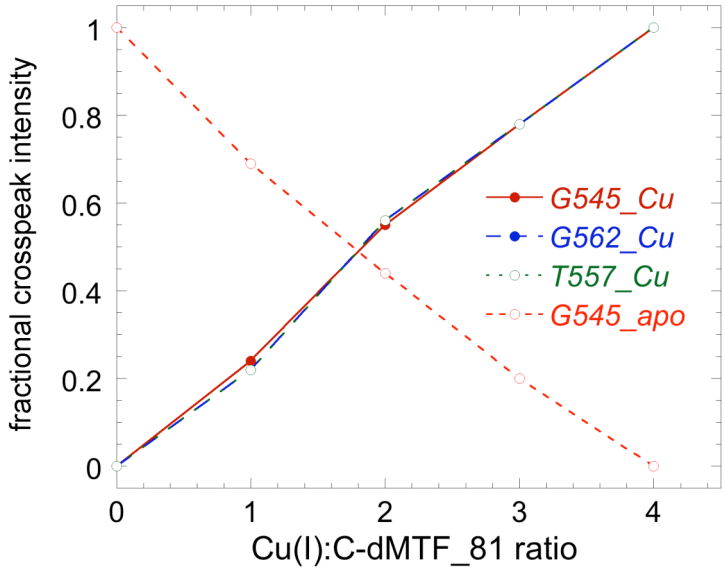

References

1. Laliberte, J., Whitson, L.J., Beaudoin, J., Holloway, S.P., Hart, P.J. and Labbe, S. (2004) The *Schizosaccharomyces pombe* Pccs protein functions in both copper trafficking and metal detoxification pathways. *J Biol Chem*, **279**, 28744-28755.
2. VanZile, M.L., Cosper, N.J., Scott, R.A. and Giedroc, D.P. (2000) The zinc metalloregulatory protein *Synechococcus* PCC7942 SmtB binds a single zinc ion per monomer with high affinity in a tetrahedral coordination geometry. *Biochemistry*, **39**, 11818-11829.
3. Chen, X., Agarwal, A. and Giedroc, D.P. (1998) Structural and functional heterogeneity among the zinc fingers of human MRE-binding transcription factor-1. *Biochemistry*, **37**, 11152-11161.
4. Liu, T., Ramesh, A., Ma, Z., Ward, S.K., Zhang, L., George, G.N., Talaat, A.M., Sacchettini, J.C. and Giedroc, D.P. (2007) CsoR is a novel *Mycobacterium tuberculosis* copper-sensing transcriptional regulator. *Nat Chem Biol*, **3**, 60-68.
5. Mustre de Leon, J., Rehr, J.J., Zabinsky, S.I. and Albers, R.C. (1991) *Ab initio* curved-wave x-ray-absorption fine structure. *Phys Rev B Condens Matter*, **44**, 4146-4156.

6. Delaglio, F., Grzesiek, S., Vuister, G.W., Zhu, G., Pfeifer, J. and Bax, A. (1995) NMRPipe: a multidimensional spectral processing system based on UNIX pipes. *J Biomol NMR*, **6**, 277-293.
7. Liu, T., Reyes-Caballero, H., Li, C., Scott, R.A. and Giedroc, D.P. (2007) Multiple metal binding domains enhance the Zn(II) selectivity of the divalent metal ion transporter AztA. *Biochemistry*, **46**, 11057-11068.
8. Liu, T., Golden, J.W. and Giedroc, D.P. (2005) A zinc(II)/lead(II)/cadmium(II)-inducible operon from the cyanobacterium *Anabaena* is regulated by AztR, an α3N ArsR/SmtB metalloregulator. *Biochemistry*, **44**, 8673-8683.
9. Busenlehner, L.S., Weng, T.C., Penner-Hahn, J.E. and Giedroc, D.P. (2002) Elucidation of primary (α3N) and vestigial (α5) heavy metal-binding sites in *Staphylococcus aureus* pI258 CadC: evolutionary implications for metal ion selectivity of ArsR/SmtB metal sensor proteins. *J Mol Biol*, **319**, 685-701.